

Calculation Improvement of No-load Stray Losses in Induction Motors with Experimental Validation

Miloje M. Kostić¹

Abstract: On the basis of the known fact that all air gap main flux density variations are enclosed by permeance slot harmonics, only one component of stray losses in rotor (stator) iron is considered in the new classification, instead of 2 components: rotor (stator) pulsation iron losses, and rotor (stator) surface iron losses. No-load rotor cage (high-frequency) stray losses are usually calculated. No-load stray losses are caused by the existence of space harmonics: the air-gap slot permeance harmonics and the harmonics produced by no-load MMF harmonics. The second result is the proof that the corresponding components of stray losses can be calculated separately for the mentioned kind of harmonics. Determination of the depth of flux penetration and calculations of high frequency iron losses are improved. On the basis of experimental validation, it is proved that the new classification of no-load stray losses and the proposed method for the calculation of the total value is sufficiently accurate.

Keywords: High frequency no-load losses, Rotor (stator) iron no-load stray losses, Rotor cage high-frequency losses, Permeance slot harmonics, MMF harmonics.

1 Introduction

It is commonly stated that additional losses may be divided into 2 so-called no-load stray losses and stray load losses, which often tends to lead to confusion, as the origin of the stray losses is poorly defined by this classification. It is better that a clearer classification be obtained by the given definition [1, 2].

- a) The predominant source of *stray load losses* is current distribution producing a stepped *MMF* in the air gap in load regime, which is called stray load losses. The second source is slot leakage flux and overhang leakage flux, which produce fundamental frequency stray load losses. Stray-load losses (P_{LL}), as the 5th loss component, are defined as the balance of total load losses (ΣP_y) and the sum of the 4 classical load-loss components in induction motors: losses in iron (P_{Fe}), friction losses and ventilation (P_{fw}), losses in stator-coil (P_{CuS}) and losses in rotor

¹University of Belgrade, Electrical Engineering Institute “Nikola Tesla”, Serbia; E-mail: mkostic@ieent.org

conductors (P_{CuR}). Total load losses are determined from a direct load test, and “stray load losses” is the difference $\Sigma P_\gamma - (P_{Fe} + P_{fw} + P_{CuS} + P_{CuR})$.

- b) Stray losses in the no-load regime are *no-load stray losses*. They occur predominantly due to the main flux distribution differentiation referred to as ideal sinusoidal distribution, called *no-load stray losses*. These flux variations are due to the permeance variation along the machine gap. These losses are included in the total core losses measured by a no-load test on induction motors. Stray no-load losses components due to the fundamental frequency are very small ($\leq 5 - 10\%$).

The no-load stray (high-frequency) losses in the nonskewed induction motor may be subdivided into the following components [1 – 5]:

- (i) *No-load stray (high-frequency) losses in stator iron* (instead of a) stator-teeth pulsation losses; and b) stator core surface losses; according to the classical classification;
- (ii) *No-load stray losses in rotor iron* (instead of c) rotor-teeth pulsation losses; and d) rotor core surface losses; according to the classical classification;
- (iii) *No-load stray losses in rotor cage*.

The first 2 components are called *additional iron losses*, and component (iii) is *no-load stray (high-frequency) losses in the rotor cage*.

The stray losses occur due to imperfect insulation between the bars and rotor iron existing only when the rotor slots are skewed.

The high-frequency iron losses are connected to the air gap flux density variation due to permeance variation along the machine gap. High-frequency losses in the stator core are usually assumed to be negligible, since the rotor slot openings are small. Stray (high-frequency) iron losses are in a thin layer of metal at the surface laminations. No-load stray losses in the rotor cage exist due to rotor tooth flux pulsation and the corresponding induced bar currents. The classical calculation procedure for determining no-load cage losses owing to rotor tooth flux pulsation is presented in [6, 7].

Components (ii) and (iii) are the most important ones, the high-frequency losses, which make more than 90% of no-load high frequency losses [4 – 9]. The no-load high-frequency losses are caused by rotor revolution and the existence of the following high-harmonic fluxes:

- the air-gap slot permeance harmonics; and
- the high harmonics, produced by no-load MMF.

Since no-load stray losses and basic iron losses appear simultaneously in the no-load test, it is difficult to distinguish one from another, as their variation is similar [4]. However, no-load high-frequency losses may be measured separately by the measurement method, which is now described briefly.

2 Calculation of Magnetomotive Force Harmonics and Permeance Slot Harmonics

High-harmonics are to be determined first, and then the rotor cage high-frequency losses and rotor (stator) core surface losses are calculated. Generally, the 2 most important types of flux density slot harmonics in the induction machines air-gap are:

- a) Flux density harmonics (B_{fh}), due to MMF harmonics, produced by the steps in the stator load current distribution, i.e. no-load current (I_0) produced the high harmonic (B_{Fh0}).
- b) Permeance slot harmonics ($B_{P,ks/p}$), which are the result of the slot openings, exist even when the MMF is purely sinusoidal.

2.1 Harmonics of the magnetomotive force and the corresponding flux density harmonics

The peak values of MMF harmonic (Fh) are given by:

$$F_1 = \frac{3}{p\pi} K_{d1} K_{p1} \sqrt{2} I_1 w_1 \quad (1)$$

The peak value of the MMF fundamental harmonic (1st order harmonic), for the machine with $p = 1$, is

$$F_1 = \frac{3}{p\pi} K_{d1} K_{p1} \sqrt{2} I_1 w_1, \quad (2)$$

where $w_1 = 2pw_s$, q_1 is the number of turns per phase. Then, the peak values of the MMF harmonic (F_h), may expressed per unit of the fundamental harmonic (F_1), i.e.

$$\frac{F_h}{F_1} = \frac{1}{h_f} \frac{K_{dh} K_{ph}}{K_{d1} K_{p1}}. \quad (3)$$

The peak values of the flux density harmonics are:

$$B_{fh} = \frac{3}{p\pi} \frac{\mu_0}{g K_{gh} K_{Sh}} \frac{K_{dh} K_{ph}}{h_f} \sqrt{2} I_1 w_1 \quad (4)$$

where:

μ_0 – magnetic permeability of the air gap,

g – air gap length,

K_{gh} – air gap (Carter) factor (usually it is considered that $K_{gh} = K_{g1}$),

K_{Sh} – magnetic circuit saturation factor.

For the saturation factor, it is often taken into account that $K_{Sh} = K_{S1}$ (i.e. as for the fundamental harmonic), though the influence of saturation is different for different harmonics. While the magnetic path of the higher harmonics lies in

the air gap and the tooth tops, the magnetic path of the lower harmonics also comprises the teeth and core of the stator and the rotor. On the basis of that and [11, 12], in the methodology applied in this paper:

a) for the air gap (Carter) factor

- $K_{gh} = 1$, for harmonic order $h \geq S/p+1$, and
- $K_{gh} = K_{g1}$, for harmonic order $h \leq S/p-1$,

b) for the magnetic circuit saturation factor

- $K_{gh} = 1$, for harmonic order $h \geq S/p+1$, and
- $K_{Sh} = K_{s1}$, for harmonic order $h \leq S/p-1$,

where S/p is the number of stator slots per pair pole.

The flux density slot harmonics due to MMF harmonics, whose order is $h_f = 5, 7, 11, 13, S_1/p-1, S_1/p+1, \dots, 2S_1/p-1, 2S_1/p+1, kS_1/p+1$, is usually expressed per unit of the fundamental harmonic ($B_{f1} = 1$ pu):

$$\frac{B_{fh}}{B_{f1}} = \frac{1}{h_f} \frac{K_{dh}}{K_{d1}} \frac{K_{ph}}{K_{p1}} \frac{K_{gh}}{K_{g1}} \frac{K_{sh}}{K_{s1}}. \quad (5)$$

For the field slot harmonics whose order $h_f = kS_1/p\pm1$, (5) becomes:

$$\frac{B_{f,kS/p\pm1}}{B_{f1}} = \frac{1}{kS/p \pm 1} \frac{K_{gh}}{K_{g1}} \frac{K_{sh}}{K_{s1}} \quad (6)$$

c) as distribution factor and pitch factor, have a value as for the first harmonic, $K_{d,kS/p\pm1} = K_{d1}$ and $K_{d,kS/p\pm1} = K_{d1}$.

2.2 Permeance slot harmonics

The effect of core saliency, a toothed surface opposite to the air gap, on the magnetic flux density (B) is shown in Fig. 1, as the distribution of the flux density, within the slot pitch. Since the $B(\alpha)$ wave form is symmetrical about the centre of the slot pitch, its Fourier series contains only a constant component and cosine terms [10, 11]. Every pulsation field harmonic can be presented as the sum of revolving field waves with amplitudes half as large. The first is forward revolving and the second is backward revolving. The amplitude of these revolving slot harmonics, of order $kS/p\pm1$, is given by following equation [5, 6, 11]:

$$B_{P,kS/p\pm1} = (\beta / 2) K_{g1} B_{med} A_k. \quad (7)$$

To determine the magnitude of these parameters: β , K_{g1} , A_k and B_{med} , it is necessary to find $g(x)$, the effective air-gap length as a function of position around the air-gap. The seminal work in this respect was published by Carter in 1926 [13]. Using the method of conformal transformation, an analytical method was developed for calculation of the flux density as a function of position along

the smooth rotor surface facing a multiplied-slotted stator surface when a constant magnetic potential exists between them. Such a distribution is readily resolved into its harmonic components from which the air-gap permeance coefficients may readily be extracted. Further, Carter's method calls for an iterative solution to determine certain geometry-based constants, requiring the repeated use of elliptic functions and integrals.

At the time, when most calculations were carried out using a slide-rule, this proved to be an insurmountable barrier. As a consequence of this, much effort was subsequently expended into devising approximations to Carter's method, some of which are summarised in [11, 12]. On the basic systematic results in Freeman's paper [14], the mentioned approximate method [11, 12] was found to be valid over a wide range, and it will be used for slot permeance harmonic calculations here. The magnitude of these mentioned parameters, β , K_{g1} , A_k and B_{med} , are determined:

- $B_{med} = B_1$ is the medium value of the flux density (B_{med}) is the amplitude of the fundamental harmonic in the air gap (B_1),
- K_{g1} is air gap (Carter) coefficient is defined as [10 – 13]:

$$K_g = t_s / (t_s - 1.6 \beta s). \quad (8)$$

- Coefficient β , which is defined as ratio:

$$\beta = (B_{\max} - B_{\min}) / (2B_{\max}) \quad (9)$$

and is calculated by following equation [10 – 12]:

$$\beta = 0.43(1 - e^{-(s/g - 0.7)/3.3}) \quad (10)$$

- Values of coefficient A_k are given by [11, 14]:

$$A_k = \frac{2}{\pi k} \frac{\sin(1.6 \pi k s / t_s)}{1 - (1.6 k s / t_s)}, \quad k = 1, 2, 3, 4. \quad (11)$$

Its values depend on the rate s/t_s , i.e. from geometry s and t_s (Fig. 1).

Table 1
Tabular presentation of the dependence $A_K = f(s/t_s)$.

s/t_s	0.2	0.25	0.3	0.35	0.4	0.45	0.50
A_1	0.598	0.721	0.825	0.911	0.976	1.012	1.039
A_2	0.488	0.520	0.509	0.460	0.384	0.311	0.194
A_3	0.339	0.283	0.194	0.098	0.020	-0.02	-0.04
A_4	0.192	0.097	0.015	-0.03	-0.03	-0.01	0.01
A_5	0.077	0.002	-0.02	-0.01	0.008	0.011	9E-08

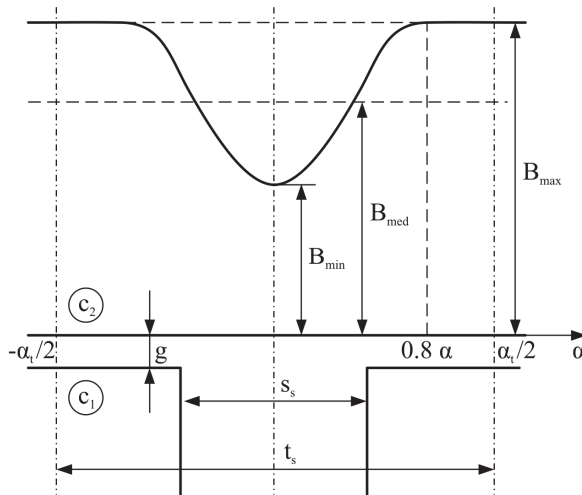


Fig. 1 – Distribution of the magnetic flux density (B) in the air gap within the slot pitch length (τ_s).

2.3 Resulting amplitude of slot harmonics in no-load condition

The slot permeance harmonics ($B_{P,kS/p\pm 1}$) produced by the fundamental harmonic MMF are at a standstill with respect to the slot harmonics ($B_{f,kS-p\pm 1}$), created by the corresponding slot harmonic MMF, but they are a phase displaced. This displacement exists for 2 reasons:

1. The coordinate origin for the MMF slot harmonics corresponds to the phase winding axis, which passes through the tooth centre or the slot centre depending on the coil pitch (y_c), while the coordinate origin for the slot permeance harmonics given by (5) is in the slot centre.
2. High harmonics of the magnetomotive force (MMF) and the corresponding flux density are in the time phase with the stator current (I_1), while the permeance slot harmonics are in the phase with the resultant MMF and the resultant current $\bar{I}_1 + \bar{I}_2 = \bar{I}_0$, i.e. the last is in the phase with the no-load current (I_0).

As analysis shows for the no-load condition, the permeance slot harmonics are in the time phase with the MMF slot harmonics.

In the addition to the same order of slot harmonics of both kinds, slot permeance harmonics have to be deduced on the phase winding axes. This means that the permeance slot harmonic amplitudes of the first and second order ($k = 1, 2$), which have a negative value in the slot centre (Fig. 1 and (12)), have to be multiplied by -1 in the case when the phase winding axis corresponds to the slot centre. If the phase winding axis is the tooth centre, then the permeance slot harmonic amplitudes of the first order ($k = 1$) have to be multiplied by 1 ,

and the permeance slot harmonics of the second order ($k=2$) by -1 . These conclusions are valid for both harmonics of the same pair, i.e. for harmonics of order $kS/p+1$ and $kS/p-1$.

Harmonics of MMF and flux density corresponding to the same pair, i.e. harmonics of the order $h_f = kS/p+1$ and $h_f = kS/p-1$ always have amplitudes of the opposite sign, because the pitch factor (K_{ph}) for one slot harmonic has a positive sign, and for the other slot harmonic of the same pair has a negative sign. Signs of distribution factors (K_{dh}) are the same for both harmonics of the same pair.

The resultant amplitude of slot harmonics of the same order, in the no-load condition, is determined as the sum of both harmonics, permeance slot harmonics and MMF slot harmonics, i.e.:

$$B_{ho,kS/p\pm1} = B_{po,kS/p\pm1} \pm B_{fo,kS/p\pm1}. \quad (12)$$

Sign “+” in the sum (17) is always associated with slot harmonics of one order, and sign “-“ for the other two harmonics of order $k6q\pm1$.

On the basis of this precise analysis, for two slot harmonics of the first order ($k=1$), it is established that the resultant amplitudes can be determined by the equations:

$$B_{S/p-1} = B_{P0,S/p-1} + B_{f0,S/p-1}, \quad (13)$$

$$B_{S/p+1} = B_{P0,S/p+1} - B_{f0,S/p+1}. \quad (14)$$

In the no-load condition, harmonic values ($B_{P0,kS/p\pm1}$) are considerably greater than the values of the harmonics ($B_{f0,kS/p\pm1}$) for the same orders ($h_f = kS/p\pm1$), (equations (6) and (7), and **Table 1**). Consequently, the corresponding values ($B_{P0,kS/p\pm1}/B_1$) and $\Sigma(B_{P0,kS/p\pm1}/B_1)^2$ are greater than the values ($B_{f0,kS/p\pm1}/B_1$) and $\Sigma(B_{f0,kS/p\pm1}/B_1)^2$ for the same orders of harmonics (equations (6) and (7), and **Table 1**).

From the two permeance slot harmonic fields of the first order ($h_{po} = kS/p\pm1$), the one that rotates in the same direction as the motor has a sign opposite to the flux density corresponding slot harmonic, produced by MMF. The other, which rotates in the opposite direction, has the same sign as the flux density corresponding to slot harmonics. In this case, the corresponding resultants for one pair of harmonics of the same order, for example $h_{P0,S/p\pm1} = 18\pm1$, i.e. 17 and 19, are [11, 14]:

$$B_{h0,17} = B_{P0,17} + B_{f0,17}, \quad (15)$$

$$B_{h0,19} = B_{P0,17} - B_{f0,19}, \quad (16)$$

and then

$$B_{h0,17}^2 = B_{P0,17}^2 + B_{f0,17}^2 + 2B_{P0,17}B_{F0,17}, \quad (17)$$

$$B_{h0,19}^2 = B_{P0,19}^2 + B_{f0,19}^2 - 2B_{P0,19}B_{F0,19}. \quad (18)$$

Equations (17) and (18) give [15]:

$$B_{h0,17}^2 + B_{h0,19}^2 = B_{P0,17}^2 + B_{P0,17}^2 + B_{f0,17}^2 B_{f0,19}^2 \quad (19)$$

since the value $2B_{P0}B_{f0,17} - 2B_{P0,19}B_{f0,19}$ is considerably less than the value given on the right-hand side of (19).

From (19), it is concluded that the no-load losses, produced by high harmonics, will be able to divide in two parts: one, which corresponds to the permeance slot harmonics ($B_{P0,kS/p\pm 1}$) and the other, which corresponds to the MMF slot harmonics ($B_{f0,kS/p\pm 1}$). No-load losses, produced by the 1st order permeance slot harmonics ($B_{P0,S/p\pm 1}$) harmonics, are several (5–15) times greater than the corresponding losses produced by slot harmonics ($B_{f0,S/p\pm 1}$) due to MMF, in the same order.

On the basis of the proof given by (19), one can conclude that should not determine the resultant amplitudes of slot harmonics. Need only to calculate the absolute values permeance slot harmonics ($B_{P0,kS/p\pm 1}$) and slot harmonics ($B_{f0,kS/p\pm 1}$), since it is sufficient for the determination of the stray no-load losses and stray torques associated with slot harmonics. This gives an opportunity to avoid the procedure for determining the algebraic sign of slot harmonics, which is complicated [11, 12, 14 – 16].

3 Calculation of no-load higher-frequency losses

In the large induction motor with stator coils in open stator slots, high-frequency losses are a predominant constituent of total no-load losses. When high-harmonics are determined, and then calculated:

- high-frequency losses in the rotor cage, due to permeance slot harmonics and MMF high harmonics,
- high-frequency losses in the rotor and stator iron, due to permeance slot harmonics and MMF high harmonics.

3.1 Harmonics of the magnetomotive force and corresponding flux density harmonics

If the rotor is coil-wound, the rotor winding pitch and distribution factors are usually so small for the stator slot harmonics that no appreciable currents are induced in the rotor. In this case, the stator permeance slot harmonics produce flux pulsation in the rotor teeth, and formulae for such pulsation losses calculation are known.

In a squirrel-cage motor, the rotor bars in adjacent slots form a closed loop around in the intermediate tooth, so that any change in the rotor tooth flux is opposed by current in the loop, in accordance with the constant linkage theorem. Therefore, at high frequencies of the stator slot harmonics in the rotor, the net rotor tooth flux remains almost constant and the flux pulsation loss is negligible, unless the rotor slots are skewed [11, 12, 16].

If the slots are skewed one stator pitch, each rotor bar spans nearly 360° of the stator slot harmonics, regardless of the slot ratio, and the net voltage induced in each bar will be nearly zero. However, there will then be a considerable voltage acting from bar to bar at the midpoint of the core length, and this will cause the current to flow through the laminations in this region to an extent depending on the level of the bar insulation. In this case, it can be calculated that 80 – 90% of high-frequency losses are iron losses and only about 10 – 20% is due to the interbar currents [16].

In the straight rotor slots, high-frequency losses in the rotor cage occur owing to harmonics. Generally, the two most important types of flux density harmonics in the induction machines air-gap are: permeance slot harmonics and MMF high harmonics. The induced currents in the straight rotor bar can be calculated from the equivalent circuit of Fig. 2, for each type of harmonics (permeance slot harmonics or MMF harmonics) and each harmonic order (h), [11, 12, 16, 18, 19].

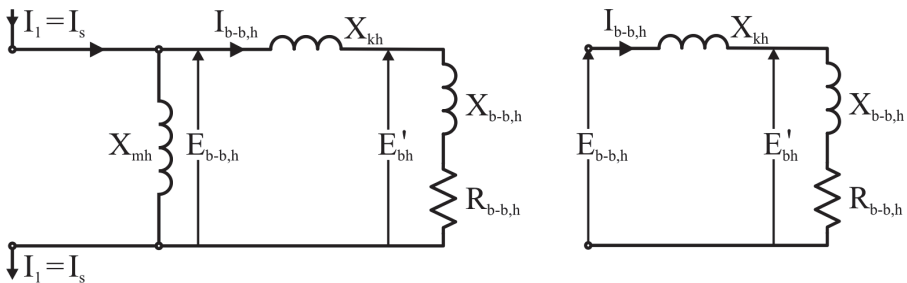


Fig. 2 – Equivalent circuit of cage induction motors bar-bar loops for high harmonics in particular, including permeance slot harmonics.

Because the harmonic magnetising reactance is much smaller than the main magnetising reactance, each harmonic terminal voltage $E_{lh} = E_{b-b,h}$ ($E_{b-b,h}$ – the corresponding harmonic electromotive force (EMF) in bar-bar loops). The RMS value of the corresponding electromotive force harmonic is:

$$E_{b-b,h} = (1/\sqrt{2})2\pi f_1 h \Delta\Phi_{b-b,h}, \quad (20)$$

where $\Delta\Phi_{b-b,h}$ is the harmonic flux through a bar-bar loop, Fig. 3.

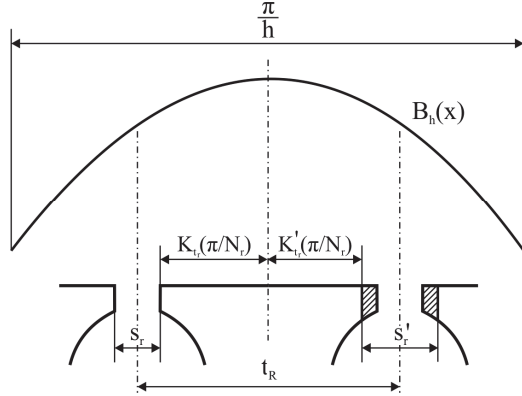


Fig. 3 – Flux-density distribution along the rotor slot pitch, for harmonic order (h).

If the flux-density distribution in relation to a rotor tooth centre is given by the expression $B_h = B_h \cos(hx)$, the flux entering the rotor tooth body (and bar-bar loops), $\Delta\Phi_{b-b,h}$, is given by the integration of the flux-density over the rotor-tooth body width:

$$\Delta\Phi_{b-b,h} = (D_r / 2)L_r B_h \int_{-K_{tr}\pi/(R/p)_l}^{+K_{tr}\pi/(R/p)} \cos(hx) dx \quad (21)$$

and the K_{tr} factor characterised rotor-tooth body width is:

$$K_{tr} = \frac{t_r - s_r}{t_r}, \quad (22)$$

where h is harmonic order, D_r is rotor outer diameter, L_r is rotor length, t_r is rotor slot pitch, s_r is slot width, R/p is the number of rotor slots per pole pair, B_h is the flux density harmonic calculated by (3) – (6) for harmonics due to MMF, and by (7) for permeance slot harmonics.

Hence, the fluxes entering the rotor tooth body (and bar-bar loops), $\Delta\Phi_{b-b,h}$, are given by the following expression:

$$\Delta\Phi_{b-b,h} = B_h (L_{Fe} t_r) \frac{2 \sin\left(\pi \frac{h}{R/p} \frac{t_r - s_r}{t_r}\right)}{\pi \frac{h}{R/p}}. \quad (23)$$

The corresponding bar-bar loops currents driven by $E_{b-b,h}$ are:

$$I_{b-b,h} = \frac{E_{b-b,h}}{\sqrt{R_{b-b,h}^2 + (X_{kh} + X_{b-b,h})^2}}, \quad (24)$$

where (see Fig 4) $R_{b-b,h}$ is the total bar-bar loop resistance, $X_{b-b,h}$ is the total bar-bar loop internal reactance, $X_{k,h}$ is the bar-bar loop leakage reactance for h^{th} harmonics.

The resistance ($R_{b-b,h}$) and reactances ($X_{b-b,h}$ and X_{bh}), see Fig. 4, are calculated by the following expressions:

$$R_{b-b,h} = \rho_b \frac{L_b}{b_b \delta_{bh}} \left(2 \sin\left(\pi \frac{h}{R/p}\right) \right)^2, \quad (25)$$

$$X_{b-b,h} = R_{b-b,h}, \quad (26)$$

$$X_{kh} = (2\pi h) \frac{\mu_0 L_r (t_r - s_r)}{g K_{gh-k} K_{Sh-k}}, \quad (27)$$

where K_{gh-k} is air gap (Carter) factor, for bar-bar loops leakage flux for h^{th} harmonics (usually it is $K_{gh} = K_{g1}$, for $R/p < S/p$) [12], K_{Sh-k} is the magnetic circuit saturation factor, for bar-bar loops leakage flux for h^{th} harmonics (usually it is $K_{gh} = K_{g1}$).

The skin effect in the end ring is much smaller, so the ring resistance may be neglected in (25).

A squirrel-cage rotor consists of R bars cast or pushed through the rotor slots and connected at both ends by end rings so that the cage is permanently shorter (R = rotor slot total number). Each phase of a squirrel-cage winding is in effect a single-turn loop composed of two adjacent bars and the intervening end-ring segment. For example, phase loop consists of bars 1 and 2 and the respective segments of the end rings. The bars carry each a current I_{b1} , I_{b2} , I_{b3}, \dots , and the end-ring segments carry each a current I_{er1} between bars 1 and 2, I_{er2} between bars 2 and 3, and so on (Fig. 4).

Obviously, the number of phases in a squirrel-cage rotor is equal to the number of bars (or loops). As the number of loops is equal to the number of bars, $N_{loops} = N_{bar} = R$, then the rotor cage high-frequency losses due to harmonics order (h) may be calculated by:

$$P_{cage,h} = 2R(R_{b-b,h} I_{b-b,h}^2), \quad (28)$$

where R is the number rotor slots (and bars), $R_{b-b,h}$ is the total bar-bar loop resistance, $I_{b-b,h}$ is bar-bar loop currents.

As each bar resistance carries two loop bar-bar loop currents ($I_{b-b,i}$ and $I_{b-b,i-1}$, Fig. 4), the factor of 2 is introduced in (28).

Generally, fluxes, electromotive forces, induced currents in the loops and bar of a squirrel-cage, corresponding resistances ($R_{b-b,h}$) and reactances ($X_{b-b,h}$ and X_{bh}) and high-frequency losses in the rotor-cage ($P_{cage,h}$) may be calculated by (20) – (28), for each type of harmonics (permeance slot harmonics or MMF harmonics) and each harmonic order (h).

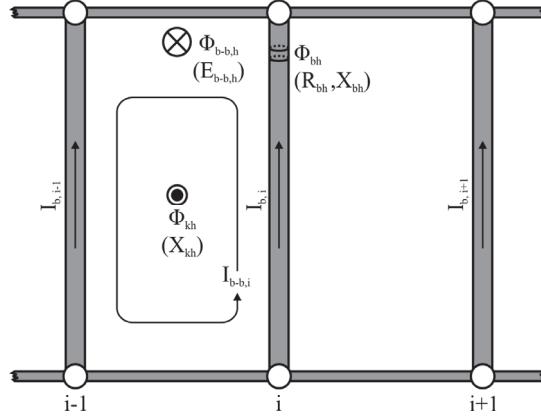


Fig. 4 – Fluxes, electromotive forces and currents in the loops and rotor bar, and corresponding resistances ($R_{b-b,h}$) and reactances ($X_{b-b,h}$ and X_{bh}).

The total high-frequency losses in the rotor-cage ($\Sigma P_{cage,h}$) due to high harmonics, may be calculated by:

$$\sum P_{cage,h} = \sum_{h_p=k\frac{S}{p}\pm 1} P_{Cage,k\frac{S}{p}\pm 1} + \sum_{h_f=k\frac{S}{p}\pm 1} P_{Cage,k\frac{S}{p}\pm 1} + \sum_{h=6k\pm 1} P_{Cage,6k\pm 1}, \quad (29)$$

where $\Sigma P_{Cage,h_p=k\frac{S}{p}\pm 1}$ is high-frequency losses due to permeance slot harmonics of order $h_p = kS/p \pm 1$, $\Sigma P_{Cage,h_f=k\frac{S}{p}\pm 1}$ is high-frequency losses due to MMF slot harmonics of order $h_p = kS/p \pm 1$, and $\Sigma P_{Cage,h=6k\pm 1}$ is high-frequency losses due to MMF belt harmonics of order $h_p = 6k \pm 1 < S/p - 1$.

From (28), all the components are calculated in the first, second and third sums on the right-hand side (29).

The high-frequency losses in the rotor-cage due to no-load MMF slot harmonics ($\Sigma P_{Cage,h_f=k\frac{S}{p}\pm 1}$) must not be neglected, although it is usually given in the literature [7, 8, 16, 18, 19]. Also high-frequency rotor-cage losses due to no-load MMF harmonics $6k \pm 1$ order ($P_{cage,6k\pm 1}$) should be taken into account.

3.2 Calculation of high-frequency losses in the stator and rotor due to MMF and permeance slot harmonics

The high-frequency losses in the rotor and stator iron occur due to slot permeance harmonics and MMF harmonics. The iron losses due to slot permeance harmonics are first investigated and usually have greater values, and they will be separately analysed in this paper. The iron losses occurring due to MMF harmonics (MMF slot harmonics and MMF belt harmonics) must not be neglected, although this is usually given in the literature [7, 8, 16, 18, 19].

As the field harmonics rotate past the rotor surface, eddy currents are induced in the rotor lamination, which cause surface I^2R power losses. For

frequencies of up to 1200 Hz, characteristic for slot harmonics ($N_S/p\pm 1$), the field penetration in silicon steel ($\mu_{Fe} = 200$) is $\delta_{Fe} = 0.3\text{--}0.4 \text{ mm} < d_{Fe} = 0.6 \text{ mm}$ for thick laminations. This means that the skin effect is not significant. Carter has shown that, if the flux pulsates through a lamination thickens d_{Fe} with a maximum flux density B_h and frequency, $f = f_1 h_f$, and if the reaction of eddy currents on the forcing flux is neglected, the eddy-current loss is given by the following relationship [6, 7]:

$$P_{Fe,h} = \left(\frac{\sigma_{Fe}}{24} d_{Fe}^2 \right) B_h^2 (f_1 h_f)^2 \left(2\pi R \ell_{Fe} \frac{R}{h} \right), \quad (30)$$

where σ_{Fe} is silicon steel electric conductance, B_h is flux density harmonic, μ_{Fe} is silicon steel relative magnetic permeability, d_{Fe} is silicon steel thick laminations, h is harmonic order, $h_f = f_h/f_1$, R is rotor outer radius and length stator steel, ℓ_{Fe} is rotor steel length.

If the rotor surface is flat and flux pulsations are undamped (an example of wound rotor motor), it has been proved [7] that the part $R_S/(S/p_1)$ presented the depth of flux penetration through rotor surface (Δ_h), i.e.:

$$\Delta_h = R / h = \lambda_h / (2\pi), \quad (31)$$

where λ_h is the field harmonic way length (i.e. the pole pitch).

As the first factor in (30), $\sigma_{Fe} d_{Fe}^2 / 24$, presented volume specific eddy-current losses, W/m³, at $B_h = 1 \text{ T}$ and $f = 50 \text{ Hz}$. Then the known specific eddy-current losses, W/kg, at $B_h = 1 \text{ T}$ and $f = 50 \text{ Hz}$, are:

$$p_{EC,1/50} = \frac{\sigma_{Fe} d_{Fe}^2}{24} \frac{1}{\gamma_{Fe}}, \quad (32)$$

where $\gamma_{Fe} \approx 7900 \text{ kg/m}^3$. On the basis of (29) – (31), the equation is obtained for eddy-current losses calculations, $P_{Fe,EC} = P_{Fe,sur}$

$$P_{Fe,h} = p_{EC,1/50} B_h^2 \left(h_f f_1 / 50 \right)^2 \left(2\pi R \ell_{Fe} \Delta_h \gamma_{Fe} \right). \quad (33)$$

The last factor in (33) presented core mass with surface losses, i.e. G_{Fe} [kg]

$$G_{Fe} = 2\pi R \ell_{Fe} \Delta_h \gamma_{Fe}. \quad (34)$$

From (33) and (34), the following expression is obtained:

$$P_{Fe,h} = p_{EC,1/50} B_h^2 \left(h_f f_1 / 50 \right)^2 G_{Fe}. \quad (35)$$

As the field harmonics rotate past the rotor surface, accordingly [8], we may call it rotational magnetisation. In the case of rotational magnetisation, the rotating \mathbf{B} vector can be depicted as the sum of two pulsation magnetic flux density vectors equal in peak value to the magnitude of the rotating \mathbf{B} vector, that is $|\mathbf{B}|$. If we write the magnetic flux density in the case of rotational

magnetisation as the sum of 2 pulsation components, we shall see that the eddy-current loss in this case is twice as great as the eddy-current loss in pulsation magnetisation for the same peak value of magnetic flux density (which is irrespective of the magnetic flux density). On the basis of that and (35), the expression for calculation of surface losses due to 2 revolving permeance slot harmonics order $S/p\pm 1$, is given as:

$$P_{Fe,h} = 2 p_{EC,1/50} B_h^2 \left(h_f f_1 / 50 \right)^2 G_{Fe}. \quad (36)$$

For squirrel induction motors with flux pulsations damped in the rotor iron, it is arbitrarily assumed [8, 12] that the depth of flux penetration ($\Delta_{Fe,h}$) is

$$\Delta_{Fe,h} = \lambda_h / 16, \quad (37)$$

i.e. about 40% of the value given by (31). Therefore, corresponding loss values are only 40% of the value given by (32) – (36).

We have supposed that the depth of flux penetration ($\Delta_{Fe,h}$) is

$$\Delta_{Fe,h} = h_{b0} + \lambda_h / 16 \leq \lambda_h / (2\pi), \quad (38)$$

where h_{b0} is the distance of the rotor bar top from the rotor outer surface.

When $h_{b0} \geq \lambda_h / (2\pi) - \lambda_h / 16$, then

$$\Delta_{Fe,h} = \lambda_h / (2\pi) = \Delta_h, \quad (39)$$

as it is the case with the analysed motor.

The amplitudes of these revolving MMF harmonics are calculated:

- for all MMF harmonics, whose order $h_f = 5, 7, 11, 13, 17, 6k\pm 1$, by (5), i.e. by the following equation:

$$B_{fh} = B_{f1} \frac{1}{h_f} \frac{K_{dh}}{K_{d1}} \frac{K_{ph}}{K_{p1}} \frac{K_{gh}}{K_{g1}} \frac{K_{sh}}{K_{s1}}, \quad (40)$$

- for MMF slot harmonics, whose order $h_f = kS_1/p\pm 1$, by (11), i.e. by the following equation:

$$B_{f,kS/p\pm 1} = B_{f1} \frac{1}{kS/p\pm 1} \frac{K_{gh}}{K_{g1}} \frac{K_{sh}}{K_{s1}}, \quad (41)$$

where K_{gh} is air gap (Carter) factor [12, 20] (for which usually is considered $K_{gh} = K_{g1}$), K_{Sh} is the magnetic circuit saturation factor.

The amplitude of these revolving permeance slot harmonics, order $h_{p0} = kS/p\pm 1$, is given by (12).

To determine the magnitude of these parameters: β , K_{g1} , A_k and B_{med} , it is necessary to find $g(x)$, the effective air-gap length as a function of position around the air-gap (see 2.2).

The total iron rotor (surface) losses are calculated as the sum

$$P_{Fe,HF} = \sum_{h=6k\pm 1} P_{Fe,6k\pm 1} + \sum_{h_{p_0}=kS/p\pm 1} P_{Fe,kS/p\pm 1} + \sum_{h_f=kS/p\pm 1} P_{Fe,kS/p\pm 1}. \quad (42)$$

All components $P_{Fe,6k\pm 1}$ in the first sum on the right-hand side of (42) and all components $P_{Fe,kS/p\pm 1}$ in the second and third sum on the right-hand side of (42), are calculated by (36).

The rotor core surface losses due to *MMF* harmonics (*MMF* slot harmonics) must not to be neglected, although it is usually included in literature [7, 8, 16, 18, 19]. It will be shown that the rotor iron (surface) losses (and the stator iron losses) should be determined as sum losses due to permeance slot harmonics, $kS/p\pm 1$ order (and $kR/p\pm 1$), at least for $k = 1, 2$ and 3 (some time for $k = 1 - 5$).

4 Calculation of No-load Higher-frequency Losses - Example: Large Motors with Open Slots

High-frequency losses are a major constituent of total no-load losses in the large power motor. The presented procedure for no-load high-frequency losses is examined in the example of the large induction motor with stator open slots of large power (1200 kW, 690 V, 1259 A, $2p = 6$). High-frequency no-load losses (P_{HF0}) are measured by a simple method [5, 10] described in an earlier section, so that the obtained value is $P_{HF0} = 9062$ W. It is interesting that the designer engineers' calculating value was $P_{HF0,calc} = 6200$ W. The result of our calculation is $P_{HF0,calc} = 8763$ W, i.e. only an error of 3.3% (Table 2, $P_{HF0,cal} = \Sigma(1-6) = 8763$ W).

The described method of calculation was applied to the mentioned induction squirrel-cage motors with open stator slots [20]: 2 SEZKIT 423 L-6 1200 kW, 690 V, 1259 A, $2p = 6$, $S = 72$ slots and $R = 58$ slots. The complete procedure includes calculation of the following components of high-frequency no-load losses, for harmonics order $k \leq 3$:

a) The stator core surface losses,

1. $P_{Fe,hP=kR/p\pm 1}$ – due to permeance slot harmonics (for $k \leq 5$)

b) The rotor core surface losses

2. $P_{Fe,hP=kS/p\pm 1}$ – due to permeance slot harmonics, for $k \leq 4$;

3. $P_{Fe,hf=kS/p\pm 1}$ – due to MMF slot harmonics, for $k \leq 5$;

c) The rotor cage high-frequency losses,

4. $P_{Cage,hP=kS/p\pm 1}$ – due to permeance slot harmonics, for $k \leq 3$,

5. $P_{Cage,hf=kS/p\pm 1}$ – due to MMF slot harmonics, for $k \leq 3$, and

6. $P_{Cage,hf=6kS\pm 1}$ – due to MMF belt harmonics, order $6k\pm 1 < S/p-1$.

The results of this calculation are given in **Table 2**.

Table 2

Induction motor 2SEZKIT 423 L-6 1200 kW, 690 V, 1259 A, 990 min⁻¹.

<i>The stator core HF losses</i>	$k = 1$	$k = 2$	$k = 3$	$k = 4$	$k = 5$	$\text{Sum}(\Sigma)$
1. $P_{Fe,hP=kS/p\pm 1}$	63	101	70	49.6	27.23	310.8
The rotor iron HF losses						
2. $P_{Fe,hP=kS/p\pm 1}, \Delta_{Fe,h}$ (31) $\Delta_{Fe,h}$ (37)	4218 (1656)	232 (91)	21 (8)	1.27 (0.51)		4472.3 (1755.5)
3. $P_{Fe,hP=kS/p\pm 1}$ a) $\Delta_{Fe,h}$ (31) b) $\Delta_{Fe,h}$ (37)	187 (73.4)	165 (64.8)	110 (43.2)	44.13 (17.4)	31.33 (12.3)	537.4 (211.1)
The rotor cage HF losses						
4. $P_{\text{Cagee},hP=kS/p\pm 1}$	2080	160	13			2253
Sum $\Sigma P_{HF0(1\div 4)}$ [W] [%]	6548 74.7	658 7.5	214 2.4			7420 6.2
5. $P_{\text{Cage,hf}=kS/p\pm 1}$	290	172	6			468
Sum $\Sigma P_{HF0(1\div 5)}$ [W] [%]	6838 78.03	830 9.64	375 4.36			8043 93.4
6. $P_{\text{Cage,hf}=6kS\pm 1}$	338	229	3			570
$P_{HF0,cal}=\Sigma(1\div 6)$ [W] [%]	7176 81.9	1059 12.1	375 4.3	95 1.1	58.5 0.6	8763 100

5 Improvement Calculation Method

On the basis of results in **Table 2**, it can be concluded that:

- When account the high-frequency losses

– for permeance slot harmonics first order only ($k = 1$), it is

$$\Sigma P_{HF0(1\div 4)} = 6548 \text{ W} = 74.7\% \Sigma P_{HF0(1\div 4), k=1}$$

and this value is approximatively equal to the designer calculating value (i.e. $P_{HF0,calc} = 6200 \text{ W}$).

– for permeance slot harmonics and MMF slot harmonics first order only ($k = 1$), it is obtained $\Sigma P_{HF0(1\div 5)} = 6838 \text{ W} = 78.03\% \Sigma P_{HF0(1\div 5), k=1}$, and

– for permeance slot harmonics and MMF slot harmonics first order $k = 1$, and belt harmonics (5 and 7) it is $\Sigma P_{HF0(1\div 5)} = 7176 \text{ W} = 81.9\% \Sigma P_{HF0(1\div 6), k=1}$.

- When the high-frequency losses for permeance slot harmonics and MMF slot harmonics are of first and second order ($k = 1$ and 2), and first and second order belt harmonics (order 5, 7, 11 and 13) it is obtained

$$\Sigma P_{HF0(1\div 5)} = 8235 \text{ W} = 94.0\% \Sigma P_{HF0(1\div 6), k=1\div 2},$$

and it is sufficiently accurate.

3. When $\Delta_{Fe,h}$ is calculated by (37), instead of (31), lower values (for 3097 W) are obtained for rotor iron losses, i.e. $\Delta P_{Fe,hP=kS/p\pm1} = 4471 - 1755 = 2716$ W and $\Delta P_{Fe,hf=kS/p\pm1} = 537.4 - 211.1 = 326.3$ W.
4. On the basis of points 1 and 2, it may be concluded:
 - that the components of high-frequency losses should be calculated for all slot harmonics order $k \leq 3$, and
 - that the rotor iron surface losses ($P_{Fe,hf=kS/p\pm1}$) should be calculated for the depth of flux penetration ($\Delta_{Fe,h}$) determined by (38), instead of by (37).

6 Conclusion

On the basis of experimental validation it is proved that the new classification of no-load high-frequency losses and the proposed method for the calculation of the total value (and their component) is sufficiently accurate.

No-load stray losses are caused by existence of space harmonics – the air-gap slot permeance harmonics and the harmonics produced by no-load MMF harmonics. The essential finding is the proof that the corresponding components of stray losses can be calculated separately for the mentioned harmonics. Determination of depth of flux penetration and calculations of high frequency iron losses are improved.

Acknowledgments

The author gratefully acknowledges the financial support of the Ministry for Education, Science and Technology of Serbia under the project TR33017 (from 2011–2015) and Corporation *ATB SEVER, Subotica*, Serbia, for the results of the experimental investigation.

References

- [1] K.K. Schwarz: Survey of Basic Stray Losses in Squirrel-Cage Induction Motors, Proceedings of IEE, Vol. 111, No. 9, Sept. 1964, pp. 1565 – 1574.
- [2] A.A. Jimoh, S.R.D. Findlay, M. Poloujadoff: Stray Losses in Induction Machines: Part I, Definition, Origin and Measurement, IEEE Transactions on Power Apparatus and Systems, Vol. PAS-104, No. 6, June 1985, pp. 1500 – 1505.
- [3] A.A. Jimoh, S.R.D. Findlay, M. Poloujadoff: Stray Losses in Induction Machines: Part II, Calculation and Reduction, IEEE Transactions on Power Apparatus and Systems, Vol. PAS-104, No. 6, June 1985, pp. 1506–1512.
- [4] B.J. Chalmers, J. Richardson: Investigation of the High Frequency No-Losses in Induction Motors with Open Stator Slots, Proceedings of IEE, Vol. 113, No. 10, Oct. 1966, pp. 1597 – 1605.
- [5] B.J. Chalmers: Electromagnetic Problems of A.C. Machines, Chapman and Hall, London, UK, 1970.

- [6] B. Heller, V. Hamata: Harmonic Field Effects in Induction Machines, Elsevier Scientific, Oxford, UK, 1977.
- [7] I. Boldea, S.A. Nasar: The Induction Machine Handbook, CRC Press, London, UK, 2002.
- [8] P.L. Alger, G. Angst, E.J. Davies: Stray-Load Losses in Polyphase Induction Machines in Squirrel-Cage Windings, Transactions of the American Institute of Electrical Engineers – Part III - Power Apparatus and Systems, Vol. 78, No. 3, April 1959, pp. 349 – 355.
- [9] A. Ivanov-Smolensky: Electrical Machines, Mir Publishers, Moscow, Russia, 1982. (In Russian).
- [10] M. Kostic: New Method for Estimation of Stray-Load Loss in Induction Motors, International Review of Electrical Engineering, Vol. 5, No. 2, April 2010, Part A, pp. 447 – 453.
- [11] V.I. Radin et all.: Standard Series of Induction Motors Interelektron, Energoatomizdat, Moscow, Russia, 1990. (In Russian).
- [12] F.W. Carter: The Magnetic Field of a Dynamo-Electric Machine, Journal of the Institution of Electrical Engineering, Vol. 64, No. 359, No. 1926, pp. 1115 – 1138.
- [13] E.M. Freeman: The Calculation of Harmonics, due to Slotting, in the Flux Density Wave Form of A Dinamo – Electric Machine, Proceedings of IEE - Part C: Monographs , Vol. 109, No. 16, Sept. 1962, pp. 581 – 588.
- [14] M. Kostic: The Calculation of the Flux Density's Slot Harmonics in (Un)Saturated Induction Machines, International Aegean Conference on Electrical Machines and Power Electronics, Kusadasi, Turkey, 27-29 June 2001, pp. 117 – 122.
- [15] N. Christofides: Origin of Load Losses in Induction Machines with Cast Aluminum Rotors, Proceedings of IEE, Vol. 112, No. 12, Dec. 1965, pp. 2317 – 2332.
- [16] M.M. Liwschitz: Differential Leakage of a Fractional-Slot Winding, Electrical Engineering, Vol. 65, No. 5, May 1946, pp. 314 – 320.
- [17] P.L. Alger: Induced High-Frequency Currents in Squirrel-Cage Windings, Transactions of the American Institute of Electrical Engineers - Part III - Power Apparatus and Systems, Vol. 76, No 3, April 1957, pp. 724 – 729.
- [18] B.J. Chalmers, C.K. Narain: High-Frequency No-load Losses of Cage Induction Motors, IEEE Transaction on Power Apparatus and Systems, Vol. 89, No. 6, July 1970, pp. 1043 – 1049.
- [19] F. Taegen, R. Walczak: An Experimentally Verified Prediction of the Harmonic Fields of Squirrel Cage Induction Motors, Electrical Engineering, Vol. 66, No. 4, July 1983, pp. 233 – 242. (In German).
- [20] Induction Motors 2.SRZKIT 423 Lk-6 1200 kW, 690V – Results of No-load High Frequency Losses Measurement, ATB SEVER, Subotica, Serbia. (Manufacturer document).